

Multisite observations of the PMS δ Scuti star V351 Ori^{★,★★}

V. Ripepi¹, M. Marconi¹, S. Bernabei^{2,3}, F. Palla⁴, F. J. G. Pinheiro⁵, D. F. M. Folha⁵, T. D. Oswalt⁶, L. Terranegra¹, A. Arellano Ferro⁷, X. J. Jiang⁸, J. M. Alcalá¹, S. Marinoni², M. J. P. F. G. Monteiro⁵, M. Rudkin⁶, and K. Johnston⁶

¹ INAF-Osservatorio Astronomico di Capodimonte, Via Moiariello 16, 80131 Napoli, Italy

² INAF-Osservatorio Astronomico di Bologna, Via Ranzani 1, 40127 Bologna, Italy

³ Departamento de Astrofísica, Universidad de La Laguna, Avda. Astrofísico F. Sánchez sn, 30071 La Laguna, Spain

⁴ INAF-Osservatorio Astrofisico di Arcetri, Largo E. Fermi, 5, 50125 Firenze, Italy

⁵ Centro de Astrofísica da Universidade do Porto, Rua das Estrelas, 4150-762 Porto, Portugal

⁶ Florida Inst. Technology, 150 W Univ. Blvd., Melbourne, FL 32901-6988, USA

⁷ Instituto de Astronomía, UNAM, Apdo. Postal 70-264, México D.F., CP 04510, México

⁸ National Astronomical Observatories, Chinese Academy of Sciences, Beijing, 100012, PR China

Received 5 September 2002 / Accepted 20 June 2003

Abstract. We present the results of multisite observations spanning two years on the pre-main-sequence (PMS) star V351 Ori. A total of around 180 hours of observations over 29 nights have been collected, allowing us to measure five different periodicities, most likely related to the δ Scuti variability of V351 Ori. Comparison with the predictions of linear nonadiabatic radial pulsation models put stringent constraints on the stellar parameters and indicate that the distance to V351 Ori is intermediate between the lower limit measured by Hipparcos (210 pc) and that of the Orion Nebula (450 pc). However, radial pulsation models are unable to reproduce all of the observed frequencies with a single choice of (M_* , L_* , and T_{eff}), suggesting the presence of additional nonradial modes.

Key words. stars: variables: δ Scuti – stars: oscillations – stars: pre-main sequence – stars: fundamental parameters – stars: individual: V351 Ori

1. Introduction

δ Scuti stars are usually associated with the main-sequence (MS) or post-MS evolutionary phases. To date, about ten intermediate-mass pre-main-sequence (PMS) stars have been found to pulsate with timescales typical of δ Scuti variables and a growing interest in these young objects has developed in the last few years (see Marconi et al. 2001, hereafter M01; Marconi et al. 2002, hereafter M02, and references therein). The first two candidates were discovered by Breger (1972) in the young cluster NGC 2264. The existence of PMS δ Scuti stars was later confirmed by observations of the short term variability of the Herbig Ae stars HR 5999 (Kurtz & Marang 1995) and HD 104237 (Donati et al. 1997).

The initial evidence has stimulated the theoretical investigation of the PMS instability strip, based on nonlinear convective hydrodynamical models (Marconi & Palla 1998). As a result, the topology of the instability strip for the first three radial modes was identified and a list of possible PMS pulsating candidates, mainly Herbig Ae stars, was selected on the basis of their spectral types. Then, a series of observing runs has been carried out searching for δ Scuti-type photometric variations with periods of minutes to a few hours and amplitudes less than a few tenths of a magnitude among those stars inside or close to the theoretical instability strip. These studies have confirmed the δ Scuti variability of HD 104237 (Kurtz & Muller 1999), HR 5999 (Kurtz & Catala 2001), and eight additional candidates have been identified (see Kurtz & Muller 2001; M01; M02, Ripepi & Marconi 2003).

Among the new discoveries, V351 Ori is a particularly interesting object. The star is characterized by strong long-term photometric variations, attributed to extinction by circumstellar dust clouds. This property has been considered a sign of youth, signaling the transition from an active PMS phase to the arrival on the main sequence. Similar behavior has been observed in other well known Herbig Ae stars, such as BN Ori, LkH α 234 and UX Ori (e.g., Herbst & Shevchenko 1998). The spectral properties of V351 Ori include the presence of H α emission

Send offprint requests to: V. Ripepi, e-mail: ripepi@na.astro.it

* Based on observations collected at the: Loiano Observatory (Italy), San Pedro Martir Observatory (México), OGS at Teide Observatory (Spain), JKT at Roque de los muchachos Observatory (Spain), Beijing Astronomical Observatory (China), SARA Observatory at Kitt Peak, which is owned and operated by the Southeastern Association for Research in Astronomy.

** Table 3 in only available in electronic form at <http://www.edpsciences.org>

Table 1. List of telescopes and instruments involved in the multisite campaign.

Observatory	Telescope	Instrument	Comp. Star
SAAO (S. Africa)	0.5 m	Modular Photometer	HD 290826
Roque de los Muchachos (Spain)	1.0 m JKT	SITe2 2048 \times 2048 CCD	HD 290826
Beijing Astronomical Observatory – BAO (China)	0.85 m	Three Channel Photometer	HD 290826
Loiano (Italy)	1.5 m	Three Channel Photometer (TTCP)	HD 290826
San Pedro Martir – SPM (Mexico)	1.5 m	Danish (<i>uuby</i>) Photometer	HD 290826
Kitt Peak National Observatory (USA)	0.9 m SARA	512 \times 512 CCD	HD 38248
Teide (Spain)	1.0 m OGS	1024 \times 1024 CCD	HD 38248

Table 2. Properties of V351 Ori and comparison stars.

Star	AR (J2000)	Dec (J2000)	V (mag)	Sp. T.
V351 Ori	05 44 18.8	+00 08 40.4	8.9	A7
HD 38248	05 44 23.8	+00 05 08.2	9.0	A3
HD 290826	05 44 00.4	+00 15 33.0	10.0	F5

and a pronounced inverse P Cygni profile (van den Ancker et al. 1996), the SI λ 1296 Å and OI λ 1304 Å ultraviolet lines (Valenti et al. 2000), and a broad infrared excess (van den Ancker et al. 1997). Altogether, these features clearly reveal an active phase of interaction with the circumstellar environment. On the other hand, the possibility that V351 Ori is a post-MS star has been put forward in the literature. Evidence in this sense comes from the lack of a reflection nebulosity, the absence of dense molecular gas around the star, and a space velocity which indicates that the star is approaching Orion and hence is not kinematically linked to the star forming region. Spectral analysis of hydrogen absorption lines also show some peculiarities (Koval'chuck & Pugach 1998; see also M01 for details). Recently, on the basis of high dispersion echelle spectra, Balona et al. (2002, hereafter BKW) have provided further evidence that V351 Ori is indeed a PMS star.

As already remarked, the interest for V351 Ori lies in the fact that it pulsates. Marconi et al. (2000) and M01 have interpreted the frequencies observed in the light curve of V351 Ori as due to pulsations in a mixture of several radial modes. In particular, in M01 four of the six observed frequencies have been simultaneously reproduced by a linear nonadiabatic pulsation model with mass $M_* = 1.8 M_\odot$, luminosity $L_* = 13.87 L_\odot$ and effective temperature $T_{\text{eff}} = 7350$ K. However, the comparison of the observed periods with model predictions could not help distinguishing whether the star is in the PMS or post-MS evolutionary phase of its evolution, even if the solution is consistent with the distance determined by Hipparcos. The latter, if correct, implies that V351 Ori is much closer than the Orion complex.

Owing to the short temporal coverage of our previous observations, the published periodicities are subject to the problem of one cycle per day aliasing and to a high noise level, rendering their determination rather uncertain. With the aim of overcoming this observational limitation, we have organized a multisite campaign on V351 Ori involving telescopes located in

five different countries. In this paper, we present the results of this campaign. The organization of the paper is the following: in Sect. 2 we present details on observations and data reduction; the frequency analysis is reported in Sect. 3 and results are compared with those obtained in other works and with the predictions of pulsating models in Sect. 4; the conclusions close the paper.

2. Observations and data reduction

Six observatories were involved in the observational campaign. They are listed in Table 1 together with the telescopes and instruments used. The observations have been supplemented by data obtained at the SAAO during the same period (see BKW). Two comparison stars (HD 38248 and HD 290826) have been used during the observations, depending on the constraints set by the different instruments (e.g by the field of view of the CCD etc.). Some information on these objects is given in Table 2, along with the same data for V351 Ori. For completeness, the last column of Table 1 indicates the comparison star used at each telescope.

The multisite observations on V351 Ori were performed in the Johnson *V* filter over around 2 years. We can divide the campaigns in: 1) winter 2001 (Sept. 2001–Feb. 2002); 2) winter 2002 (Oct.–Dec. 2002). In total, we gathered about 180 hour of observations over 29 nights. The detailed log of the observations is given in Table 3.

2.1. Details on single site observations

The observations obtained at SAAO are described in BKW. Considering the BAO and Loiano observations, in both cases the instrument was a three channel photometer (see www.bao.ac.cn for the BAO instrument and www.na.astro.it/~silvotti/TTCP.html for the TTCP in Loiano). These instruments allow the simultaneous observation of the variable and comparison stars, as well as the sky. Thus, the time sampling can be very short: for V351 Ori we adopted an exposure time of 10 s.

Observations in SPM were carried out using the six channel spectrophotometer (see 132.248.3.38/Instruments/danes/photomdan.html) which can simultaneously operate the *uuby* filters. For V351 Ori, we used only the *y*-band data after the proper conversion into the Johnson *V* band.

Concerning CCD observations, below we report the data acquisition and reduction in detail.

2.2. Roque de los Muchachos observations

The observations with the 1.0 m JKT (La Palma, Canary Islands, Spain) were carried out during November–December 2001 using the JAG CCD camera equipped with the 2048×2048 pix² SITe2 detector, providing a 11×11 arcmin² field of view and a pixel scale of 0.33 arcsec/pixel. A Johnson V-band filter was used during all observations with exposure times between 10 and 20 s (depending on airmass and seeing). When combined with the read-out time the sampling rate is decreased to about one photometric point every two and half minutes. Standard data reduction procedures were performed with IRAF. Circular aperture photometry was carried out with DAOPHOT under IRAF to find instrumental magnitudes of the simultaneously observed target and comparison stars. The adopted aperture radius was 70 pixels (23.1 arcsec) for the night of November 29, and 25 pixels (8.25 arcsec) for the nights of November 29 and December 3. Different aperture radii were used to account for the different seeing conditions.

2.3. Kitt Peak observations

V-band observations were obtained with the SARA 0.9 m automated telescope at Kitt Peak in Arizona. A little more than 42 hours of differential time-series photometry was obtained on nine nights between October 2001 and November 2002 by both on-site and remote-access observers. Images were collected using an Apogee AP7p camera with a back-illuminated SITe SIA 502AB 512×512 pixel CCD. The pixels are 24 microns square, corresponding to $0.73''$ at the telescope focal plane scale. Read out noise and gain for the camera are about 12.2 electrons (rms) and 6.1 electrons/ADU, respectively.

Integration times were typically 10–30 s (depending upon sky conditions and airmass), plus ~ 5 s readout and idle time between frames. Sky flats, dark and bias exposures were taken every night. All data was calibrated and reduced using standard IRAF routines.

2.4. Teide observations

Observations at Teide Observatory were carried out with the 1.0 m OGS Telescope equipped with a 1024×1024 pixel CCD. The pixel scale was $0.32''$ for a total field of view of $5.5' \times 5.5'$. Read noise and gain for the camera are about 5.4 electrons (rms) and 2 electrons/ADU, respectively. Typical integration times were 10–15 s, depending upon sky conditions. Sky flats, dark and bias exposures were taken every night. All data was calibrated and reduced using standard IRAF routines.

In order to homogenize the differential photometry obtained at telescopes which used different comparison stars and to overcome the consequent difficulty in obtaining a secure zero point stability, we have decided to subtract from the data

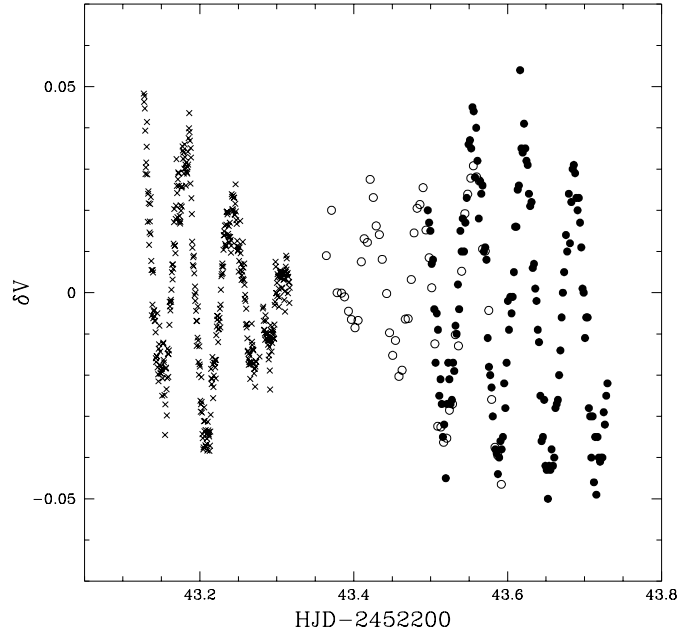


Fig. 1. Comparison between data collected during the same night (November 29, HJD = 2 452 243) at BAO (crosses), SAAO (open circles), and at JKT (filled circles).

gathered during each night at each site their mean values. This procedure will limit our analysis to frequencies longer than 1 c/d. However, since the longest time series obtained at a single site lasts around 7 h, all the frequencies lower than ~ 3.3 c/d have to be considered suspect. However, this is not a serious drawback, since the range of frequencies of interest for δ Scuti pulsations generally falls beyond this value.

In some case observations made at different observatories overlapped in time, in particular the run at SAAO and ING and/or Loiano. In this event, the data were averaged together. In order to compare the quality of the data from different sites taken at the same time, we show in Fig. 1 the observations collected at BAO, SAAO and ING during the night of November 29 (HJD = 2 452 243).

In order to have an approximately similar sampling and a similar weight for each dataset in the Fourier analysis, we had to bin the photometry obtained at BAO, Loiano, OGS and SARA. As a consequence, the total number of data points has been reduced by a factor ~ 4 . In this way, we have the significant advantage of using much less computer time for frequency extraction.

We note that, in order to improve the analysis, and in particular the phase determination, we have added to the set of observations described above the data obtained about 1 year before and described in M01. We recall that these observations were obtained at Loiano with the TTCP. These data were binned in the same manner as described above.

Finally, the light variations of V351 Ori obtained during the winter 2001 and winter 2002 campaigns are shown in Figs. 2 and 3.

3. Frequency analysis

The frequency analysis was performed using the Period98 package (Sperl 1998, www.astro.univie.ac.at/~dsn/),

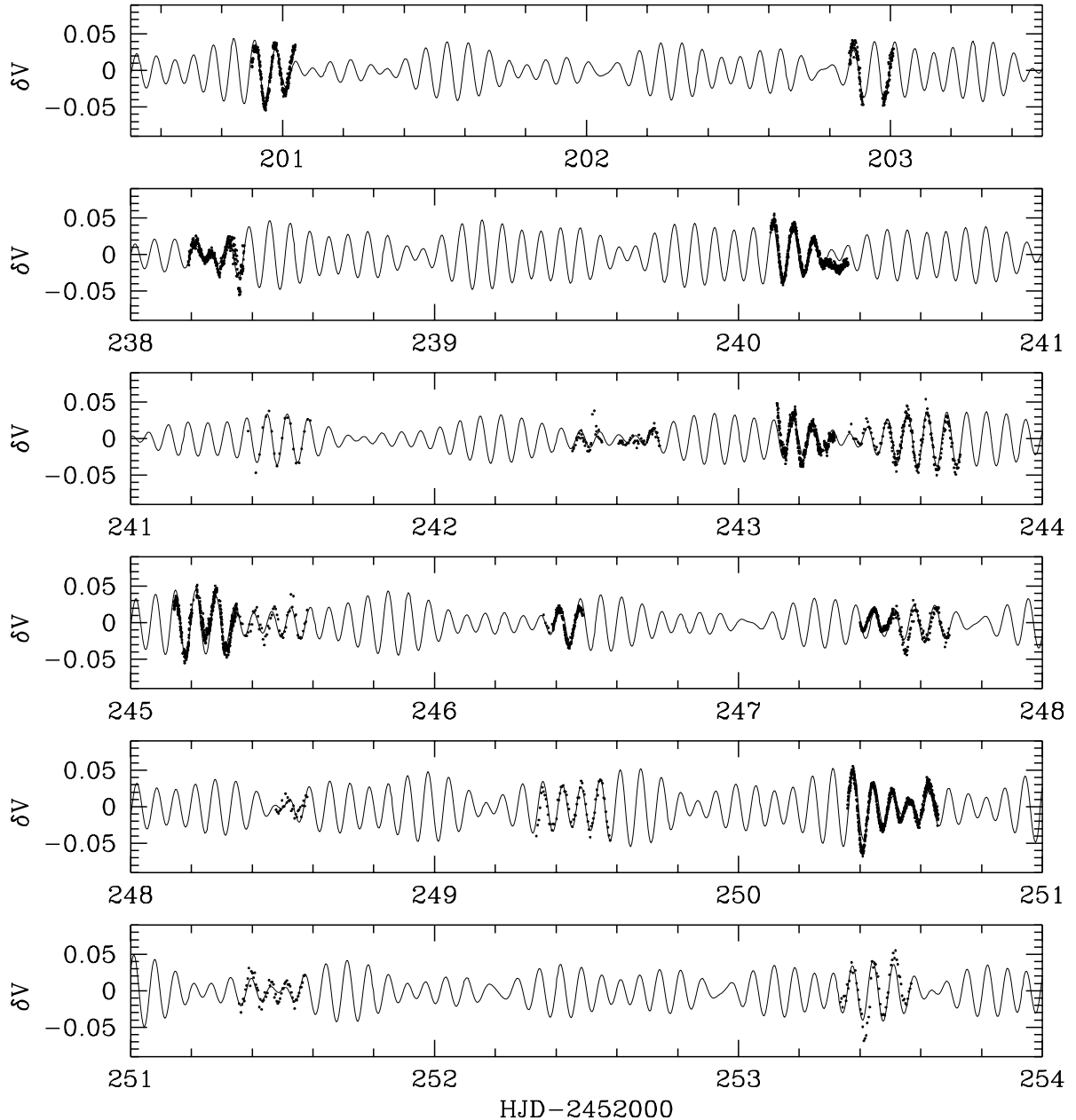


Fig. 2. Light curve of V351 Ori (points). The meaning of δV (in magnitudes) is Variable-Comparison star. The winter 2001 and winter 2002 campaigns include data from HJD = 2 452 201 to HJD = 2 452 318 and from HJD = 2 452 567 to HJD = 2 452 586, respectively. The solid line shows the fit to the data obtained as described in Sect. 3.

based on the Fourier transform method. For a better interpretation of the results, we have first calculated the spectral windows (SW) for the data set collected in winter 2001, winter 2002, and for the whole data set (which includes also the 2000 M01 data). The result is shown in Fig. 4. As can be inferred from the figure, the 1 c/d alias is not significantly reduced when analysing the whole dataset with respect to the individual sets of data (from $\sim 80\%$ to $\sim 70\%$ in amplitude). However, the main improvement obtained from analysing the whole dataset is the strong decrease of aliases between 0 and 1 c/d.

The spectral window is useful for estimating the error on the extracted frequencies. This is approximately equal to the FWHM of the main lobe in the spectral window (see, e.g.,

Alvarez et al. 1998). In our case, we find $\Delta f \sim 0.03$ c/d for the whole dataset, whereas the errors for the winter 2001 and winter 2002 campaigns are ± 0.06 c/d and ± 0.05 c/d, respectively.

Before extracting the pulsation frequencies from the time series, it is important to have a tool to identify the last significant periodicity in the data set. To this aim, we have adopted both the Scargle test (Scargle 1982, see also Horne & Baliunas 1986) and the empirical criterion suggested by Breger et al. (1993) (see also Kuschnig et al. 1997). These authors state that the signal-to-noise ratio (in amplitude) should be at least 4 in order to ensure that the extracted frequency is significant. In the following, we adopt this convention that will be referred to as “the Breger criterion”.

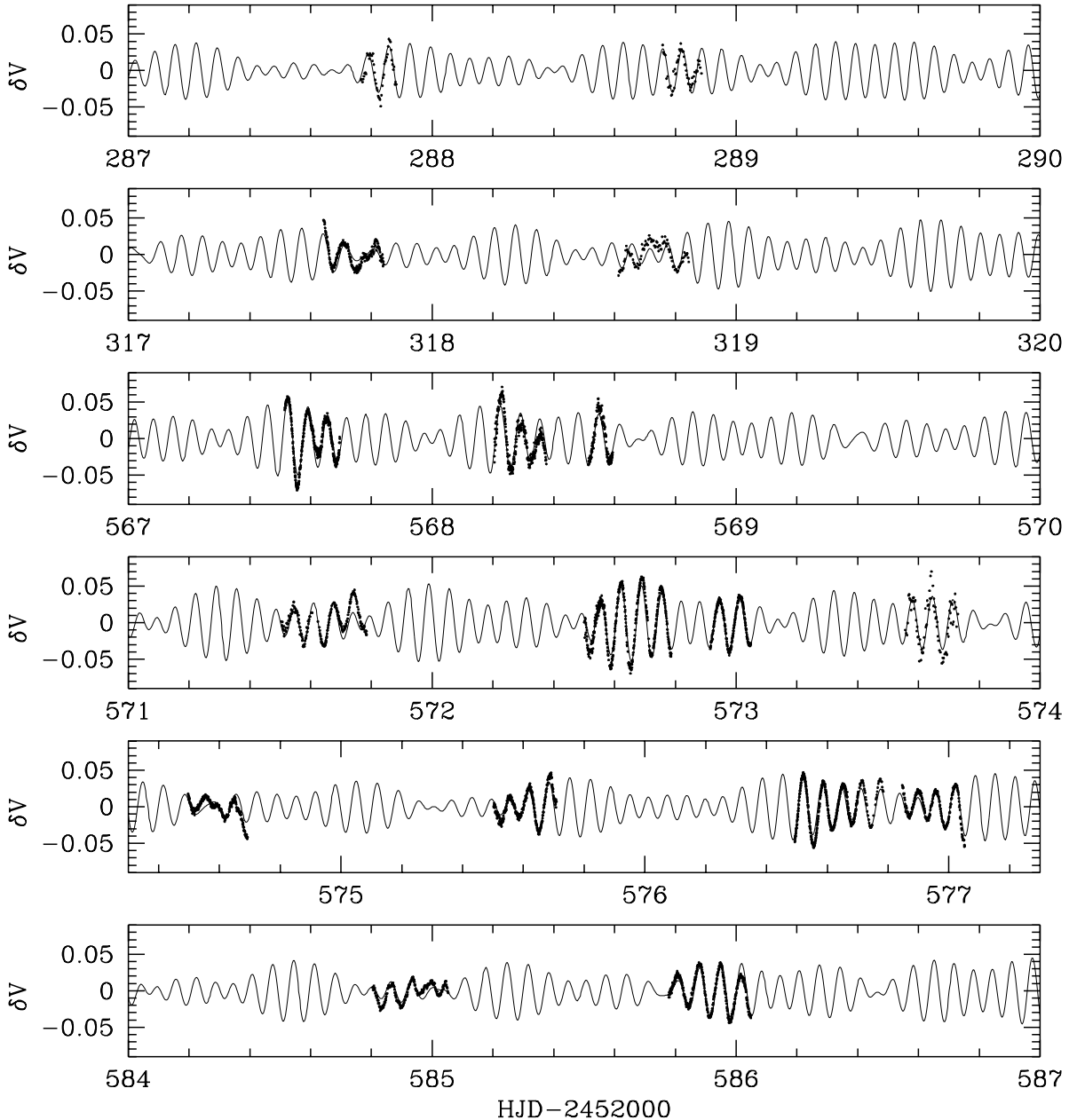


Fig. 3. Light curve of V351 Ori. Same as in Fig. 2.

In order to apply the Scargle test, we have to estimate the noise spectrum over the whole set of investigated frequencies and the number of independent frequencies in the spectrum itself. To address the first point we have used the `Period98` program to average the noise in boxes of 10 c/d width moving along the spectrum. The size of these boxes was chosen on the basis of the spectral window shape (see Fig. 4) so that at least part of the white noise was included. It is worth noting that, as recommended by Horne & Baliunas (1986), the noise spectrum used to investigate the significance of a certain frequency f_x is calculated *before* subtracting that frequency.

The second point is more difficult to address, since there is no precise way of determining the number of independent frequencies in case of unevenly spaced data (which is our case). However, as discussed in Alvarez et al. (1998), we can use the FWHM of the main lobe in the spectral window ($\Delta f \sim 0.03$ c/d

for our dataset) to estimate this value. Using Eq. (20) of Scargle (1982), we find that 99% and 90% significance levels are reached when the signal (in amplitude) is 3.9 and 3.5 times the noise. Note that the Scargle Test is, in practice, equivalent to the Breger criterion¹. In order to rely only on secure frequency detection, we choose to consider only frequencies whose level of confidence is better than 99% (i.e. $S/N = 3.9$).

Finally, we performed the Fourier analysis of the whole data set. This procedure identifies five frequencies that satisfy the above requirement. The periodograms are shown in Fig. 5, where the solid line displays the $S/N = 4$ level, and the dotted and dashed lines represent the 99% and 90% significance levels

¹ It is important to note that in Breger et al. (1993) the noise level is calculated *after* that *all* the relevant frequencies have been subtracted. To be conservative, we have adopted a noise level equal to the one used in Scargle's test.

Table 4. Frequencies, amplitudes and phases derived from the Fourier analysis of the data. Phases are calculated with respect to HJD = 24 552 500.000 The uncertainty on the frequency is ~ 0.03 c/d. The last column lists the signal-to-noise ratio (in amplitude) calculated as described in the text (see Sect. 3).

	Frequency (c/d)	Amplitude (mmag)	Phase	S/N
f_1	15.687	22.9	0.759	6.8
f_2	14.331	13.5	0.139	5.9
f_3	12.754	8.4	0.750	5.7
f_4	15.885	7.7	0.124	5.9
f_5	12.817	4.8	0.196	4.6

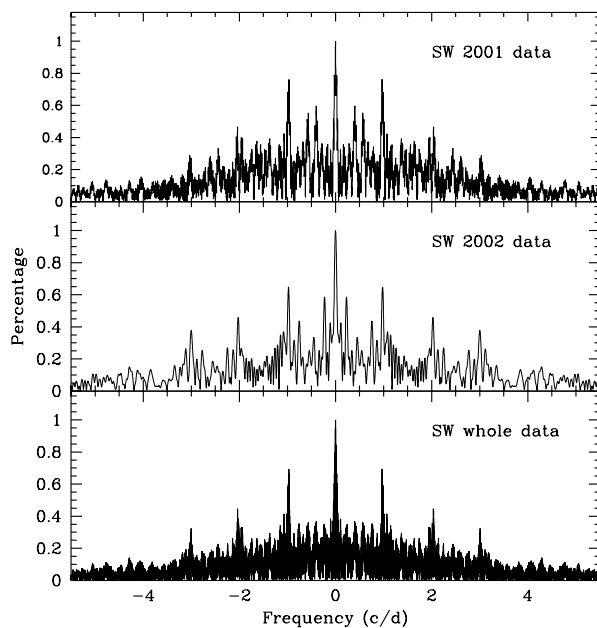


Fig. 4. Spectral window for the 2001 dataset (upper panel), 2002 dataset (middle panel), and the whole dataset (lower panel). Note that the y -axis is in amplitude units.

of the Scargle test, respectively. The derived frequencies, amplitudes, phases and relative S/N are listed in Table 4; the corresponding phase diagrams are shown in Fig. 6. A comparison between the frequencies extracted from the whole data set and those obtained during the single winter 2001 and 2002 campaigns is given in Table 5. Inspection of the table reveals that frequencies f_1 to f_4 have been detected within the errors both in the winter 2001 and 2002 campaigns, whereas f_5 is present only in the winter 2002 campaign.

We note that in Fig. 5 there is another apparently significant frequency at 3.347 c/d with $S/N \sim 3.9$. However, we do not consider it relevant to our discussion because the period of ~ 7.2 hr is just the duration of the longest time series obtained at a single site (see Sect. 2), and the resulting frequency could be a spurious artifact. Whether or not this is the case goes beyond the interest of this paper, since its inclusion in the fit has negligible influence on the results for the other frequencies, and in any case the frequency is much shorter relative to the typical values of δ Scuti stars.

Table 5. Comparison between frequencies extracted from the analysis of the winter 2001 and winter 2002 campaigns and the whole dataset. The uncertainties on the frequencies for each data set are also indicated.

	whole dataset ± 0.03 (c/d)	winter 2001 ± 0.06 (c/d)	winter 2002 ± 0.05 (c/d)
f_1	15.687	15.687	15.685
f_2	14.331	14.331	14.332
f_3	12.754	12.756	12.771
f_4	15.885	15.873	15.867
f_5	12.817	–	12.797

Table 6. Frequencies extracted in order of decreasing amplitude from the whole data set using various methods (see text). All frequencies in the table are in c/d.

Frequency	Period98	LNP (1)	LNP (2)
f_1	15.687	15.684	15.684
f_2	14.331	14.329	14.329
f_3	12.754	12.754	12.754
f_4	15.885	15.891	15.876
f_5	12.817	–	12.795

In order to test the Period98 results, we have independently carried out a frequency analysis using the Starlink Period package (`star-www.rl.ac.uk`). In particular, we used the Lomb Normalized Periodogram (LNP, Lomb 1976; Scargle 1982), noting that other algorithms, such as CLEAN (also included in Period) give results similar to those obtained with LNP.

The result of this analysis is shown in the third column of Table 6, labelled LNP (1). There is an obvious discrepancy concerning f_5 , which is not detected by LNP. To check if f_5 is reliable or not, we have adopted the following procedure: 1) we analysed the time series by means of LNP; 2) once extracted the first frequency, we used Period98 (instead of the Period package) for the fit and prewhitening; 3) the residuals from the prewhitening have been analysed again using LNP; 4) we iterated the previous steps. The result of such a procedure is shown in the fourth column (labelled as LNP (2)) of Table 6. This time the agreement with results from Period98 is almost perfect. As a conclusion, our test shows how using different packages could lead to somewhat different results, suggesting the need to use more than one method to analyse the data.

As a result of the above considerations we can conclude that the frequencies f_1 , f_2 , f_3 , and f_4 are established beyond any reasonable doubt, whereas f_5 is slightly less reliable.

The frequency f_5 deserves more discussion. In fact, it is very close to f_3 , the separation being only 0.06 c/d (we recall that the resolution for the whole data set is 0.03 c/d). As noted by Breger & Bischof (2002) close frequency pairs have important asteroseismological implications, and it is prudent to investigate whether they are real or not. In fact, there are many observational problems listed by Breger & Bischof (2002) that can lead to a false closely spaced double modes. In particular, amplitude variability of a single frequency can resemble

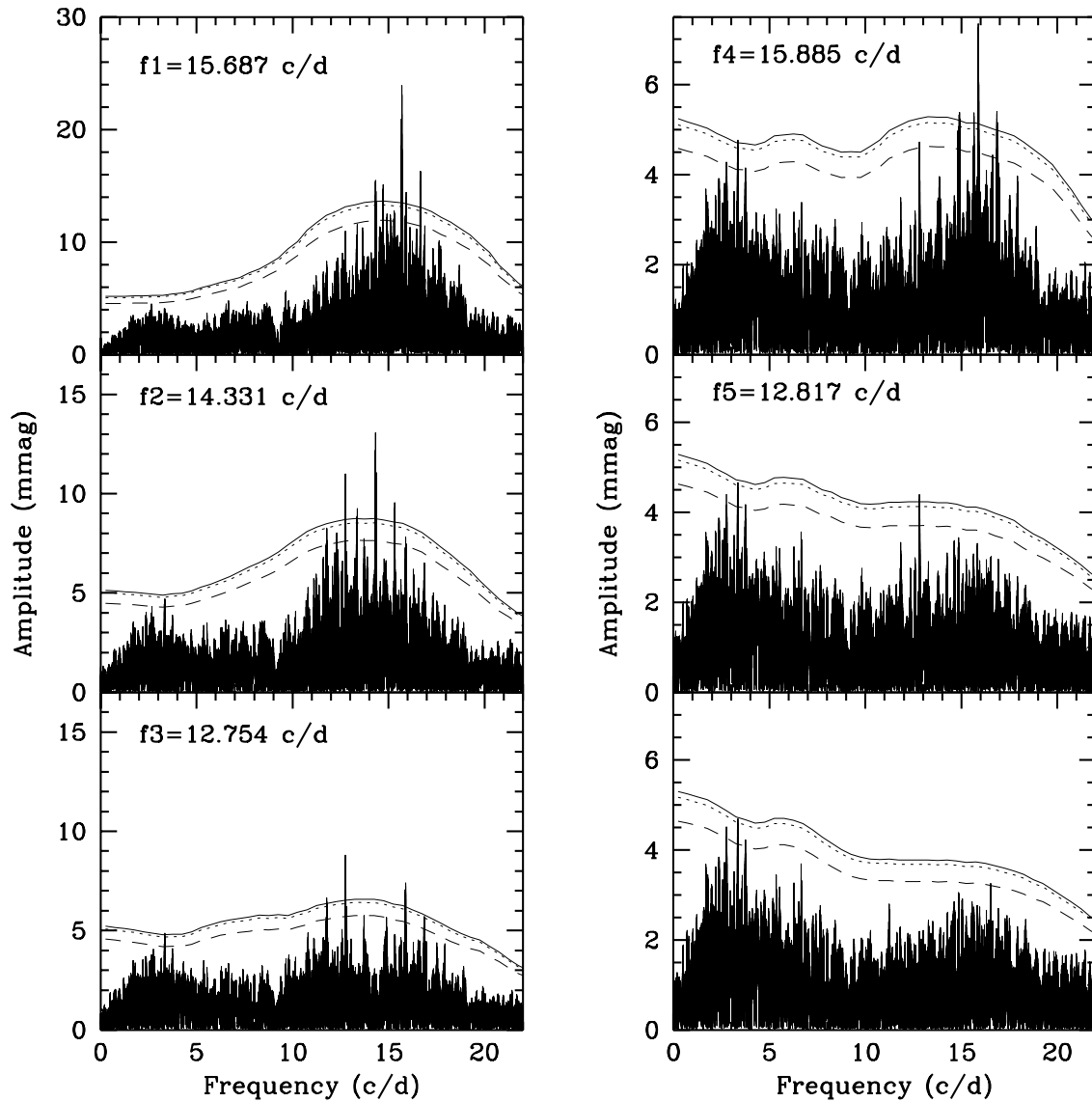


Fig. 5. Frequency analysis for the whole data set. Each panel shows the Fourier Transform after the subtraction of a pulsating frequency. The solid line corresponds to $S/N = 4$. The dotted and dashed lines show the 99% and 90% significance level calculated from the Scargle (1982) test.

the presence of a close pair. However, from the observational point of view it is very difficult to discern which hypothesis (close pair or single mode with amplitude variations) is correct. To this aim, Breger & Bischof (2002) illustrate a method which relies on the examination of amplitude and phase variation with time. However, this analysis requires a huge amount of observations while the data on V351 Ori presented here is insufficient for such a test and we simply warn the reader that f_5 might not be a real pulsation frequency.

4. Discussion

4.1. Comparison with previous work

Table 7 shows the frequencies derived in the present work, along with those found by M01 and BKW. With respect to M01, we are able to confirm within the uncertainties

only 3 frequencies: $f = 15.49$ c/d, $f = 11.89$ c/d (this is likely the -1 c/d alias of our f_3), and $f = 16.27$ c/d. Concerning the other three frequencies reported in M01, they are likely due the noise in the observations.

On the basis of the SAAO photometry and radial velocity measurements of V351 Ori, BKW have identified two and three pulsational frequencies respectively (see the last two column of Table 7). In particular they found 15.675 c/d and 14.335 c/d from the photometry and 15.682 c/d, 14.153 c/d and 11.877 c/d from radial velocities data (two of which are clearly the same as found in the photometry). BKW also performed a frequency analysis on the basis of line profile variations (see their Sect. 6 for details) that yielded a frequency at 1.90 c/d, considered highly uncertain and found indications for an additional frequency at about 20 c/d. Comparison with the BKW results (see Table 7) shows that we confirm the presence of the two

Table 7. Comparison with previous works. The labels “(P)” and “(RD)” indicate if the frequency has been detected on the basis of photometric or radial velocities data. An uncertain correspondence of previous frequencies with the present work is marked by a question mark. The uncertainties on the frequencies are also indicated.

	This work ± 0.03 (c/d)	M01 ± 0.6 (c/d)	BKW (P) ± 0.08 (c/d)	BKW (RD) ± 0.08 (c/d)
f_1	15.687	15.49	15.675	15.682
f_2	14.331	–	14.335	14.153
f_3	12.754	11.89?	–	11.877 ?
f_4	15.885	16.27	–	–
f_5	12.813	–	–	11.877 ?

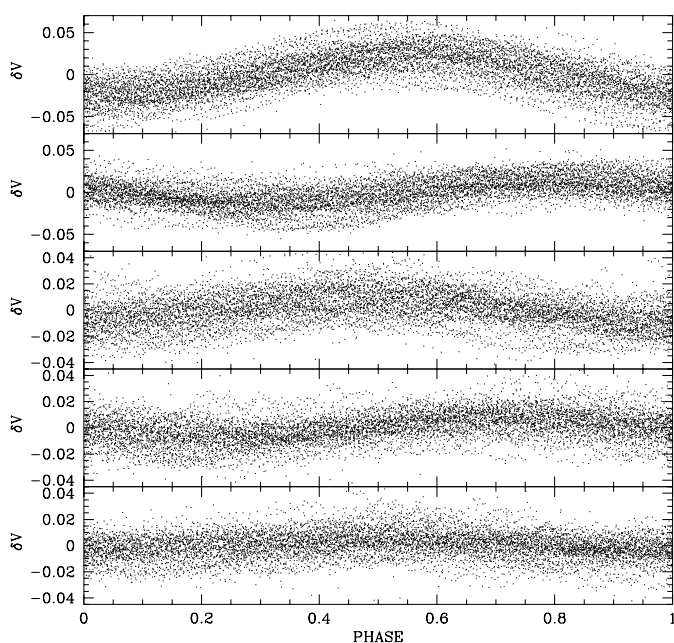


Fig. 6. Phase diagrams for the five frequencies listed in Table 4. From top to bottom the data has been phased using frequencies f_1 to f_5 .

frequencies at 15.675/15.682 c/d and 14.335/14.153 c/d (our f_1 and f_2). The third feature at 11.877 c/d could be interpreted as the -1 c/d alias of our f_3 within 2σ or of f_5 within 1σ . Alternatively, since our 1 c/d alias is not negligible, our frequency f_3 could be the alias and the frequency at 11.877 c/d the correct one. An additional hypothesis is that this frequency does not correspond neither to f_3 nor to f_5 , i.e. it is an additional pulsational frequency which shows up only with spectroscopic measurements. Concerning the remaining two periodicities reported by BKW, we do not find any power at 20 c/d and we cannot say much on the frequency at 1.90 c/d, because of our reduction technique.

4.2. Theoretical constraints

Following the same approach adopted in M01, we have tried to reproduce the five δ Scuti-like frequencies derived in the

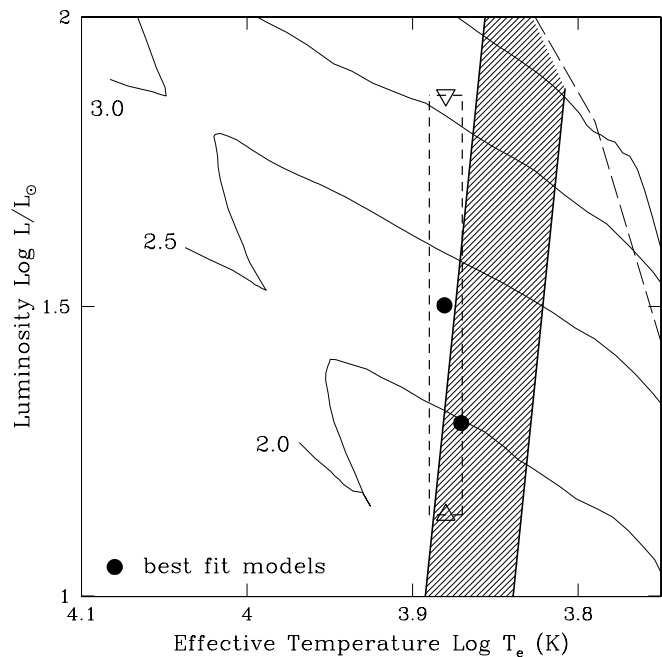


Fig. 7. Location in the HR diagram of the best fit models for V351 Ori (filled circle). The box (dashed lines and open triangles) indicates the range of luminosity and effective temperature corresponding to the empirical estimates available in the literature. Also shown are the evolutionary tracks by Palla & Stahler (1993) (solid lines), and the instability strip by Marconi & Palla (1998) (shaded area).

Table 8. Stellar parameters from the best-fit models.

Frequency	Radial mode	M_* (M_\odot)	$\log L_*$ (L_\odot)	T_{eff} (K)
f_3	first overtone	2.0	1.30	7425 K
f_1	second overtone			
f_3	second overtone	2.3	1.50	7600 K
f_1	third overtone			

previous section using linear non-adiabatic models of PMS δ Scuti stars. For each selected mass, the model luminosity and effective temperature were chosen from PMS evolutionary calculations and the constraint is provided by the observed pulsation period(s). Note that the f_1 and f_4 frequencies cannot be reproduced simultaneously since their separation is too small and comparable to the theoretical uncertainty due to the model mass zoning. The same holds for f_3 and f_5 , but, as pointed out in the previous section, the latter frequency is slightly less reliable.

On this basis, we have tried to reproduce only the three frequencies with the highest amplitude, f_1 , f_2 , and f_3 . The results show that two radial pulsation models can be found that simultaneously pulsate with frequencies f_1 and f_3 , corresponding to a mixed oscillation either in the first and second overtone or in the second and third overtone. We caution that at present we cannot indicate which of the models is the real one. The stellar parameters of the two *best fit* pulsation models are

given in Table 8 and the position in the HR diagram is displayed in Fig. 7 (filled circles). The dashed box indicates the range in luminosity and effective temperature corresponding to the empirical estimates available in the literature. The minimum luminosity comes from the Hipparcos lower limit to the distance of 210 pc (van den Ancker et al. 1998), whereas the upper limit assumes that V351 Ori is located in the Orion star forming region. The width of the box corresponds to an uncertainty of ± 0.01 dex around the mean value of $\log T_{\text{eff}} \simeq 3.88$ (van den Ancker et al. 1998). The position of the best fit models indicates that the distance of V351 Ori is intermediate between the lower limit set by Hipparcos and that of the Orion Nebula.

Despite the success in reproducing f_1 and f_3 , our radial models fail to also account for f_2 . This fact, and the inability to distinguish between f_1 and f_4 , and between f_3 and f_5 indicate that V351 Ori may be pulsating in a mixture of radial and non-radial modes, in agreement with the early suggestion of BKW. The possibility that nonradial modes might be associated with the identified frequencies clearly requires more theoretical investigation. Preliminary tests based on the comparison between observed and predicted large frequency separations (by means of scaling laws) seem to suggest that the $2 M_{\odot}$ best fit model can be compatible with the observations if we consider that f_1 and f_3 are $l = 0$ modes of consecutive mode order, whereas f_2 is a $l = 1$ mode. A similar test for the $2.3 M_{\odot}$ model suggests that in this case it is much more difficult to reconcile model predictions with the observed frequencies and frequency separations. However, these results, based on scaling considerations, need to be confirmed through the computation of specific nonradial models and we plan to address this issue in detail in a forthcoming paper.

5. Conclusions

A total of 180 hour of observations obtained during 29 nights at seven different telescopes on the PMS δ Scuti star V351 Ori have been presented. The Fourier analysis of this data set confirms the multiperiodic nature of this pulsator: we have identified five frequencies of pulsation, four of which are highly significant, while the last is more uncertain even if it is significant on the basis of both the Scargle test and the Breger Criterion.

The frequencies presented in this paper differ from those reported in M01, implying that the theoretical interpretation presented there needs to be revised. The comparison with the predictions of linear nonadiabatic radial pulsation models, in the hypothesis that the mode identification is retained, suggests that the distance to V351 Ori is intermediate between the lower limit measured by Hipparcos and the distance to the Orion Nebula. However, the fact that radial pulsation models are not able to reproduce simultaneously all the observed frequencies strongly suggests that nonradial modes might also be present. We defer a complete analysis of the pulsation modes to a forthcoming study.

Acknowledgements. We are indebted to L. Balona, C. Koen and F. van Wyk for having provided us with their data in advance of publication and in particular to C. Koen for a critical reading of the manuscript. We acknowledge R. Silvotti and L. Piau for helpful discussions. We wish also to thank the Loiano staff members for their kind support during the observations.

AAF is thankful to DGAPA-UNAM project IN113599 for financial support. FJGP acknowledges support from project ESO/FNU/43658/2001. DFMF acknowledges financial support by FCT from the “Subprograma Ciência e Tecnologia do 3º Quadro Comunitário de Apoio” and also from project POCTI/1999/FIS/34549, approved by FCT and POCTI, with funds from the European Union programme FEDER.

This work was partly supported by FCT-Portugal, through project POCTI/43658/FNU/2001.

TDO would like to acknowledge partial support for this project from NASA (grant NAGW5-9408) and NSF (AST-0097616).

References

- Alvarez, M., Hernandez, M. M., Michel, et al. 1998, *A&A*, 340, 149
 Balona, L. A., Koen, C., & van Wyk, F. 2002, *MNRAS*, 333, 923 (BKW)
 Breger, M. 1972, *ApJ*, 171, 539
 Breger, M., & Bischof, K. M. 2002, *A&A*, 385, 537
 Breger, M., Stich, J., Garrido, R., et al. 1993, *A&A*, 271, 482
 Donati, J.-F., Semel, M., Carter, B. D., Rees, D. E., & Cameron, A. C. 1997, *MNRAS*, 291, 658
 Herbst, W., & Shevchenko, V. S. 1998, *AJ*, 118, 1043
 Horne, J. H., & Baliunas, S. L. 1986, *ApJ*, 302, 757
 Koval’chuk, G. U., & Pugach, A. F. 1998, *AstL*, 24, 106
 Kurtz, D. W., & Marang, F. 1995, *MNRAS*, 276, 191
 Kurtz, D. W., & Catala, C. 2001, *A&A*, 369, 981
 Kurtz, D. W., & Müller, M. 1999, *MNRAS*, 310, 1071
 Kurtz, D. W., & Müller, M. 2001, *MNRAS*, 325, 1341
 Kuschnig, R., Weiss, W. W., Gruber, R., Bely, P. Y., & Jenkner, H. 1997, *A&A*, 328, 544
 Lomb, N. R. 1976, *Ap&SS*, 39, 447
 Marconi, M., & Palla, F. 1998, *ApJ*, 507, L141 (MP98)
 Marconi, M., Ripepi, V., Alcalá, et al. 2000, *A&A*, 355, L35
 Marconi, M., Ripepi, V., Bernabei, et al. 2001, *A&A*, 372, L21 (M01)
 Marconi, M., Palla, F., & Ripepi, V. 2002, *Comm. in Asteroseismology (Vienna)*, 141, 13 (M02)
 Palla, F., & Stahler, S. W. 1993, *ApJ*, 418, 414
 Ripepi, V., & Marconi, M. 2003, *Proc. 2nd Eddington workshop “Stellar Structure and Habitable Planet Finding”*, Palermo, 9-11 April 2003, ed. F. Favata, & S. Aigrain, (ESA SP-538)
 Scargle, J. D. 1982, *ApJ*, 263, 835
 Sperl, M. 1998, *Comm. in Asteroseismology (Vienna)*, 111, 1
 Valentí, J. A., Johns-Krull, C. M., & Linsky, J. L. 2000, *ApJS*, 129, 399
 van den Ancker, M. E., Thé, P. S., & de Winter, D. 1996, *A&A*, 309, 809
 van den Ancker, M. E., Thé, P. S., Feinstein, A., et al. 1997, *A&AS*, 123, 63
 van den Ancker, M. E., de Winter, D., & Tjin A Djie, H. R. E. 1998, *A&A*, 330, 145

Online Material

Table 3. Journal of the observations.

Starting HJD-2452000 (day)	Duration (hours)	Observatory
200.88	3.5	SARA
202.86	2.1	SARA
238.19	4.4	BAO
240.11	6.1	BAO
241.39	4.9	SAAO
242.45	7.0	SAAO+JKT
243.12	13.2	BAO+SAAO+JKT
245.14	10.6	BAO+SAAO
246.36	3.1	SAAO+Loiano
247.40	7.0	Loiano+JKT
248.48	2.5	SAAO
249.33	5.8	SAAO
250.36	7.2	SAAO+Loiano
251.36	5.2	SAAO
253.34	5.6	SAAO
287.76	2.9	SPM
288.76	3.4	SPM
317.64	4.8	SARA
318.61	5.6	SARA
567.51	4.4	Loiano
568.20	6.1	BAO+Loiano
571.50	6.4	Loiano+OGS
572.50	10.2	OGS+SARA
573.55	4.3	OGS
574.50	4.7	Loiano
575.50	5.0	OGS
576.49	12.0	OGS+SARA
584.80	6.0	SARA
585.78	6.5	SARA